Nuclear fission

Hans J. Specht

Physikalisches Institut der Universität Heidelberg, Heidelberg, Germany

The experimental evidence supporting the double-humped character of the fission barrier in actinide nuclei is reviewed and compared to theoretical predictions. The discussion covers the existence and half-life systematics of spontaneously fissioning isomers, shape-isomeric gamma decay, rotational transitions and the moment of inertia of isomers, fragment angular distributions in isomeric fission, intermediate structure in fission cross sections, and finally the systematics of barrier heights as deduced from fission probability measurements. The implications of a possible octupole deformation at the second barrier for fragment mass distributions are also discussed, including the size of the mass asymmetry and recent experiments on the competition between symmetric and asymmetric fission as a function of excitation energy.

CONTENTS

I. INTRODUCTION

The process of nuclear fission contains such a richness of different phenomena, that is barely possible to cover all of them within the framework of this review. We shall therefore restrict ourselves to a discussion of only two topics:

(a) our present understanding of the double-humped fission barrier with all its experimentally observable consequences,

(b) the possible connection between the barrier shape and fragment mass distributions, which might contain the key to the clarification of this more than thirty year old problem.

There are important reasons for this restriction. Most of the revived interest and progress in nuclear fission over the last few years has, in fact, centered around these topics. Moreover, it is in this area that fission had some effect on the rest of nuclear physics, stimulating the discussion of the general problem of binding energy of nuclei both as a function of nucleon number and nuclear shape, and leading to a phenomenon such as shape isomerism or to the prediction of the possible existence of elements beyond those known at present.

The developments to be discussed were triggered, on the experimental side, by the discovery of spontaneously fissioning isomers by Polikanov *et al.* (1962), on the theoretical side by Strutinski's attempts (1966, 1967, 1968) at a deeper understanding of the "shell correction" to the nuclear binding energy. As a short introduction and reminder of the origin of the double-humped barrier, we have therefore selected one of the first calculations of Strutinski (1966, 1967, 1968) (Fig. 1). The double-humped character of the nuclear potential energy as a function of (essentially quadrupole) deformation (thick line) arises, within the framework of the "Strutinski shell correction method" (Strutinski, 1966, 1967, 1968; Brack *et al.*, 1972), from the superposition of a macroscopic smooth liquid drop part (dashed line) and a shell correction (lower part of Fig. 1, separately for protons and neutrons), obtained from a microscopic single-particle model. Oscillations in this shell correction as a function of deformation lead to two minima in the potential energy, the normal ground state minimum at a deformation of $\epsilon_2 = 0.6$, located 2–3 MeV above the first (Sec. II). More recently, also on the basis of this macroscopic–microscopic approach, a pronounced left–right asymmetry at the outer of the two barriers has been predicted by several groups (Sec. III).

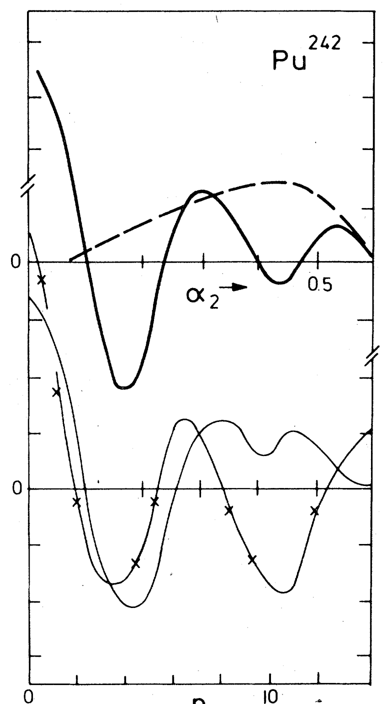

FIG. 1. Double-humped fission barrier, original drawing from Strutinsky (1966, 1967, 1968) (here, $\eta \simeq 16\,\epsilon_2$ and $\alpha_2 \simeq 2/3\,\epsilon_2$; see text for more details).

Following Strutinski's arguments (Strutinski, 1966, 1967, 1968; Brack *et al.*, 1972), the remarkable oscillatory character of the shell corrections as a function of deformation—in the same way as in function of nucleon number—is caused by variations of the single-particle level density in the vicinity of the Fermi energy. As illustrated in Fig. 2 (taken from a recent review of Nix, 1972; also Möller and Nix, 1973) for a pure harmonic-oscillator potential, single-particle levels arrange themselves in bunches or highly degenerate "shells" at any deformation for which the major to minor axis ratio c/a of the equipotential surfaces is equal to the ratio of two small integers. Nuclei with a filled shell, i.e., with a level density at the Fermi energy smaller than the average have an increased binding energy compared to the average, because the nucleons occupy deeper and more

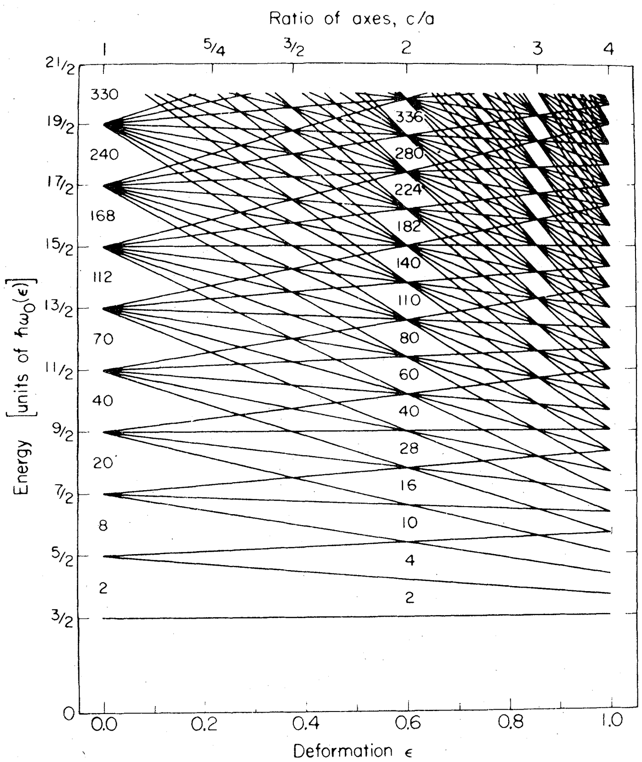

FIG. 2. Energy levels of a harmonic-oscillator potential for prolate spheroidal deformations (Möller and Nix, 1973; Nix, 1972). The particle numbers of the closed shells are indicated for a sphere and for a spheroid whose major axis is twice its minor axis.

bound states; conversely, larger level density is associated with a decreased binding energy. In an actual nucleus, the spin–orbit interaction and other corrections only change the particle numbers associated with the shells, but not their position as a function of deformation (Nix, 1972; Möller and Nix, 1973; Wong, 1970). It is therefore precisely this oscillatory behavior that is responsible for spherical or deformed ground states, secondary minima in fission barriers ($c/a = 2$), and asymmetric barrier shapes.

We do not intend here at all to review progress in theory, but refer instead to extensive recent publications (Brack *et al.*, 1972; Möller and Nix, 1973; Johansson *et al.*, 1970; Nix, 1972; Pauli, 1973). We will just list the headlines and give examples of the principal developments:

(a) A deeper understanding and, in some sense, an "*a posteriori*" justification of the Strutinski procedure, based on Hartree–Fock results (Vautherin, 1973; Flocard *et al.*, 1973; Brack and Quentin, 1973).

(b) Extensive calculations of potential landscapes on the basis of the Strutinski procedure by many groups (Strutinski, 1966, 1967, 1968; Brack *et al.*, 1972; Möller and Nix, 1973; Johansson *et al.*, 1970; Nix, 1972; Pauli, 1973; Möller, 1972; Mustafa *et al.*, 1973; Larsson and Leander, 1973), demonstrating, among many other features, the stability of the second minimum against asymmetric and γ-deformations.

(c) Studies of the dependence of the shell correction energy on nuclear temperature (Moretto, 1972; Jensen and Damgaard, 1973; Jensen and Dössing, 1973; Schmitt and Mustafa, 1973).

(d) Calculations of dynamical quantities such as moments of inertia (Sobiczewski *et al.*, 1973; Pauli and Ledergerber, 1973), mass parameters and lifetimes for spontaneous and isomeric fission (Pauli and Ledergerber, 1973), and fragment mass distributions (Maruhn *et al.*, 1973).

(e) Attempts to understand the coupling between the collective and intrinsic degrees of freedom of the system ("nuclear viscosity") (Schütte and Wilets, 1973; Wieczorek *et al.*, 1973).

II. THE DOUBLE-HUMPED BARRIER

Our approach here will be to review recent experimental progress and to present some quantitative comparisons with available calculations. The observable consequences of a double-humped fission barrier are listed in Fig. 3. Nuclei caught in the second minimum can either tunnel through the outer barrier (isomeric fission), or decay back to the first minimum (isomeric γ decay). There will be a spectrum of low-lying excited states built on the ground state in the second well, which can be studied, at least in principle, by "conventional" spectroscopic methods. Moving higher up in excitation energy to the barrier region, intermediate structure occurs in fission cross sections. It consists of mainly two types—a broad structure caused by "transmission resonances," and a fine structure seen as a clustering of neutron resonances. The detailed behavior of these cross sections together with information on isomers is used to extract barrier heights. We will discuss all these features in order of increasing excitation energy. A more extensive review of such "spectroscopy" has been given by Bjørnholm (1972).

Following any nuclear reaction exciting an actinide nucleus to energies above the fission barrier, the probabilities of prompt fission, of decay back into the first minimum and of trapping in the region of the second minimum, are of the order of 0.9, 0.1, and 10^{-5}–10^{-4}, respectively. A detailed investigation of the properties of shape isomeric states therefore meets tremendous experimental difficulties. Our present knowledge is mostly restricted to identification of isotopes, half-lives, and in some cases, excitation energies of the states decaying by spontaneous fission. According to the latest survey (Britt, 1973), the actinide region of the chart of nuclei, seen in Fig. 4, shows 33 fission isomers between ^{92}U and ^{97}Bk with half-lives ranging from 10^{-11} to 10^{-2} sec. Those are faster by 20–30 orders of magnitude than the fission half-lives of the ground states, because of the increased tunneling probability. Several cases are known of additional spin isomerism within shape isomers; these will be discussed below. The occurrence of fission isomers in this region of the chart of nuclei is in qualitative agreement with the predicted (Brack *et al.*, 1972; Möller and Nix, 1973; Johansson *et al.*, 1970; Nix, 1972; Pauli, 1973) "switch-over" in the relative heights of the two barriers: For $Z > 97$, the half-lives become too short to be observable with current techniques, for $Z < 92$ shape isomeric γ decay rather than fission presumably becomes dominant. Quantitatively, of course, the exact boundaries of this region depend on the sensitivity of experimental techniques.

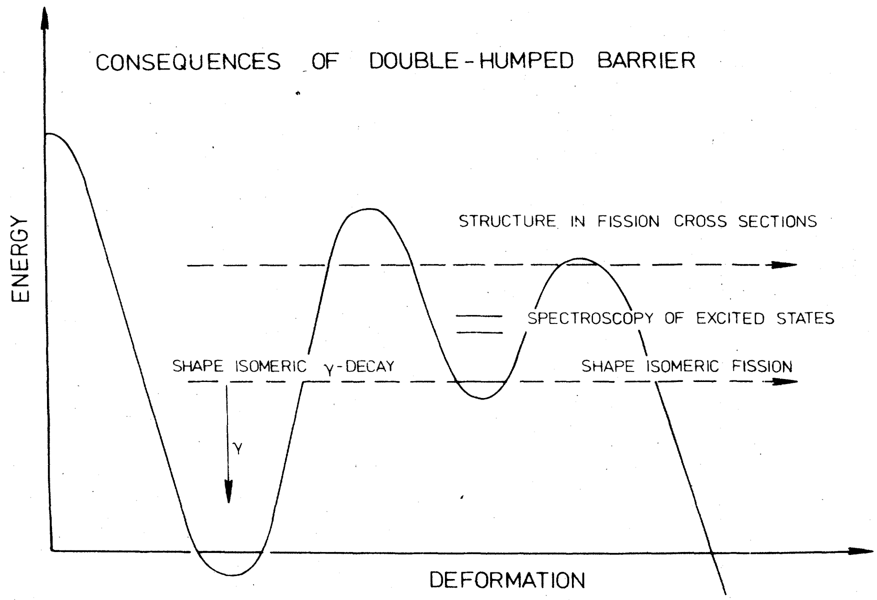

FIG. 3. Observable consequences of a double-humped barrier with two potential wells.

Do the known half-lives exhibit any systematic behavior? A plot due to Vandenbosch (1973b) of those half-lives thought to be connected with the lowest state in the second well versus neutron number is shown in Fig. 5. It includes the newest subnanosecond values for the even–even Pu isotopes, obtained in Copenhagen (Limkilde and Sletten, 1973; Metag *et al.*, 1973) by an ingenious projection method for measuring the decay of recoiling nuclei in flight. Two features in Fig. 5 are noteworthy—the striking similarity in the variation of the half-lives with neutron number for

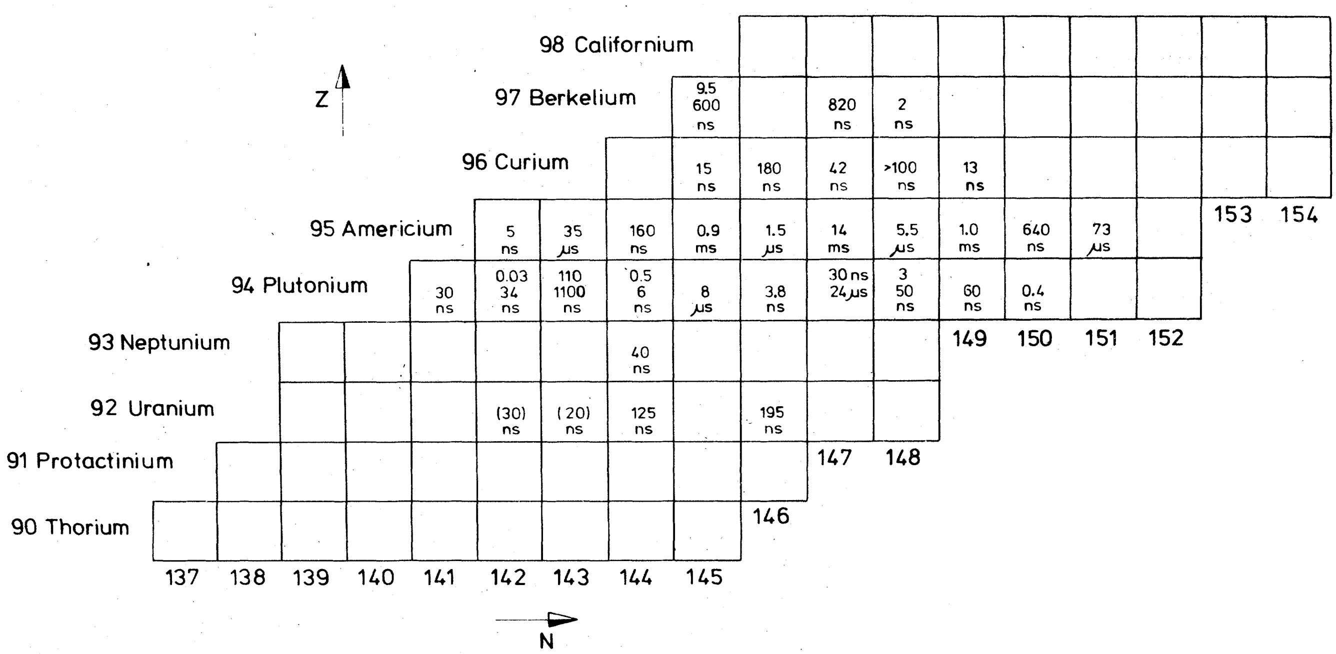

FIG. 4. Actinide region of the chart of nuclei showing the half-lives of all fission isomers known at present. Two numbers in the same field indicate the existence of spin isomers within shape isomers.

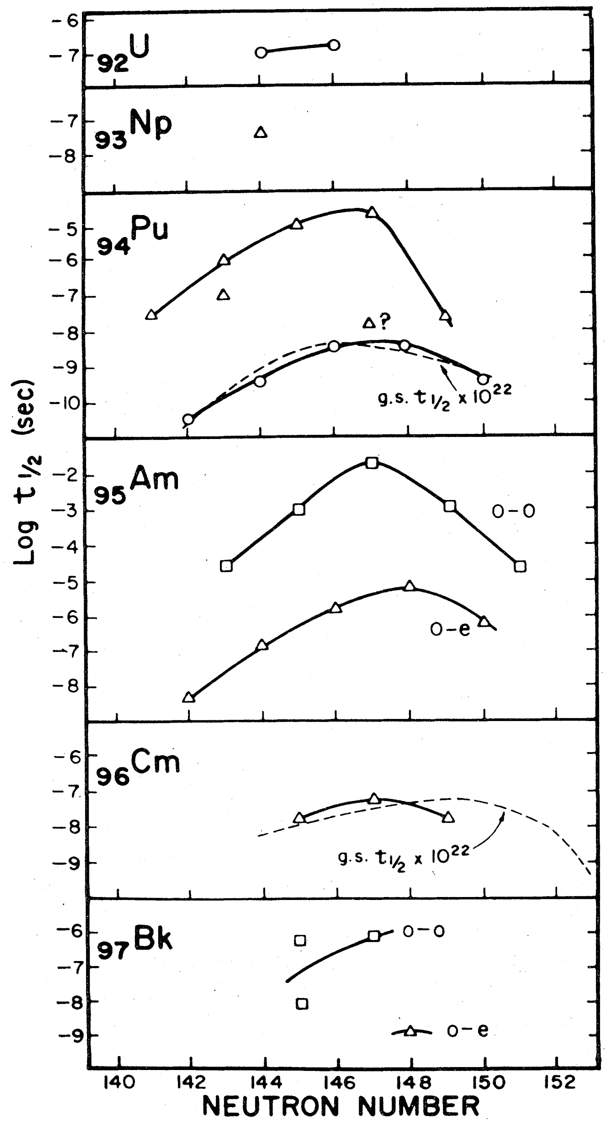

FIG. 5. Fission isomer half-lives as a function of neutron number (Vandenbosch, 1973b; data from Britt, 1973; Metag *et al.*, 1973). Circles, triangles, and squares represent values for doubly even, odd, and doubly odd nuclei. The dashed lines correspond to the observed half-lives for spontaneous fission from the ground states multiplied by 10^{22}.

doubly even, odd and doubly odd nuclei, and the very regular odd–even effect in absolute magnitude (3–4 orders per odd particle). The maximum in the variation, occurring at the neutron number $N = 146$–148, is interpreted (Vandenbosch, 1973b; Metag *et al.*, 1973) as a manifestation of the magic neutron number (strongest negative shell correction) at the deformation $c/a = 2$ associated with the second minimum, in good agreement with most of the calculations. The nature of the odd–even retardation has not yet been completely clarified. It could be caused by a change in either the barrier thickness: barrier curvature and/or effective mass, or in the barrier height, from a change in pairing energy and/or the "specialization energy" of the odd particle because of spin conservation under change of deformation. A recent review by Vandenbosch (1973b) gives an extensive discussion of the systematics in half-lives.

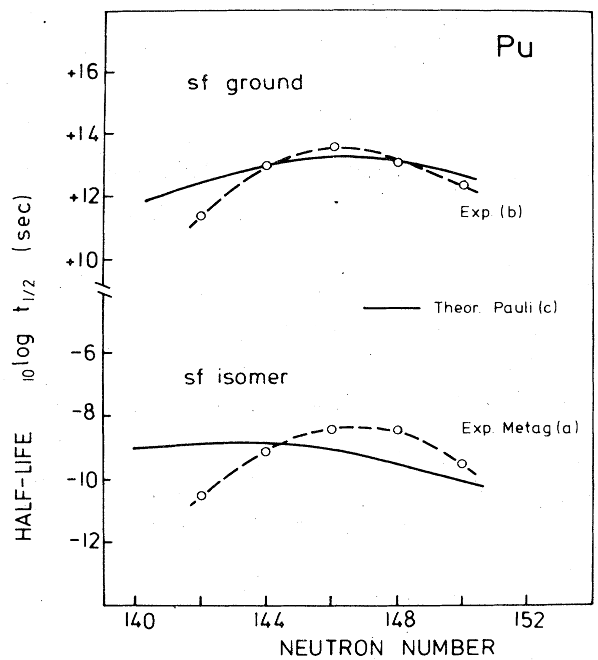

FIG. 6. Experimental [(a) (Metag *et al.*, 1973), (b) (Hyde, 1964)] and theoretical (from Pauli and Ledergerber, 1973) half-lives for spontaneous fission from the ground states and shape-isomeric states of even Pu isotopes.

A comparison between the measured half-lives and those obtained in the calculations by Pauli and Ledergerber (1973) is shown in Fig. 6, both for spontaneous fission from the ground states (Hyde, 1964) and the shape isomeric states (Metag *et al.*, 1973) of even Pu isotopes. These calculations not only contain the static potential energy surfaces, but also—within the framework of the cranking model—dynamical quantities such as the deformation-dependent effective nuclear mass involved in the tunneling through the fission barrier. The agreement over 22 orders of magnitude without any readjustment of the liquid drop or the shell correction parameters is truly remarkable. However, several problems remain. The magic neutron number for the isomers (Pauli, 1973; Pauli and Ledergerber, 1973), i.e., the neutron number associated with the largest negative shell correction at the deformation $c/a = 2$ occurs somewhat lower than obtained in other calculations (Möller and Nix, 1973) and observed experimentally. More important, the liquid drop parameters, obtained from a fit to the lifetimes of Fig. 6, do not reproduce the measured barrier heights of the Pu isotopes; nor is the agreement between theory and experiment as good for the neighboring elements without a readjustment of the parameters (Pauli and Ledergerber, 1973). Further refinements are definitely needed. As an interesting side result of the calculated variable inertia, the dynamical path in deformation space corresponding to the smallest half-life, i.e., the least-action trajectory in the WKB approximation employed, does not pass through the static saddle points of the deformation energy. The nucleus rather tunnels through the barrier at a deformation where the potential energy is higher than the saddle point energy; the corresponding points of highest energy are called "dynamical barriers" (Pauli and Ledergerber, 1973).

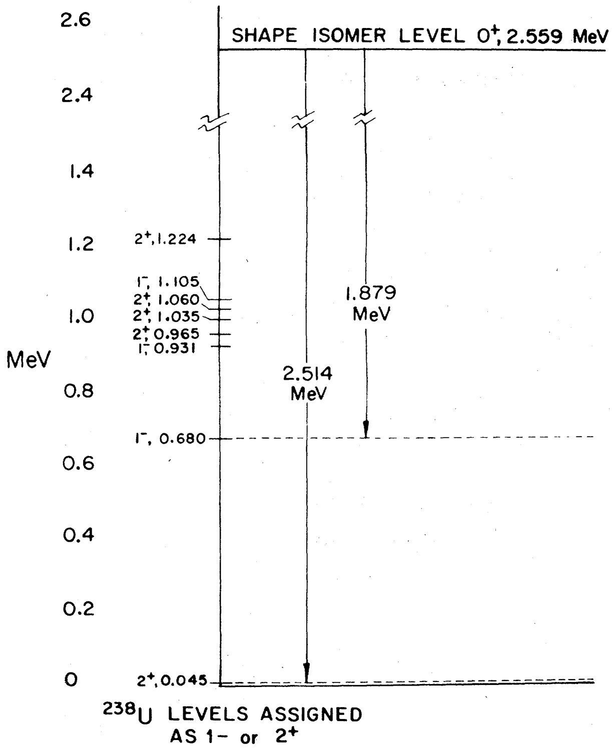

FIG. 7. Proposed decay scheme of the shape-isomeric gamma decay in ^{238}U (from Russo *et al.* 1973).

Up to very recently, the competing γ decay of the shape-isomeric states had escaped detection. Unfortunately, the investigation of such delayed electromagnetic transitions is even more difficult than that of the more "dramatic" and more efficiently measureable process of delayed fission, because of the nearly prohibitive background of delayed γ rays from fission fragments. In view of the hindrance factor of 10^7 (Nix and Walker, 1969) for the γ branch relative to fission, for equal tunnel probability through the two barriers, the best candidates for such a search are isotopes for which the penetration probability through the first barrier is much higher than that through the second; this happens in the lower Z actinides (see discussion of Fig. 4 and Fig. 14). A long-term effort by the Seattle group (Russo *et al.*, 1973) has now been rewarded with the successful identification of the γ-branch of the 200 nsec ^{238}U shape isomer. Delayed coincidences were used with a pulsed beam; the background was determined using beam energies below the threshold for populating the shape isomer. The level scheme proposed is shown in Fig. 7. Two lines were found with a half-life in agreement with that observed for the fission branch. These have been attributed to the decay of the 0^+ shape-isomeric state to the lowest 2^+ rotational and 1^- octupole levels in the first well of ^{238}U. On the basis of the observed yields, the branching ratio between γ decay and fission is estimated to be of the order of 40, consistent with the predictions for a more penetrable inner barrier (Russo *et al.* 1973) in this nucleus.

The excitation energy of 2.56 MeV for the isomeric state represents the first accurately known number for any fission isomer. Usually, this quantity is obtained rather indirectly by measuring excitation functions for isomer production, relying on uncertain and model-dependent extrapolations of the threshold behavior. The systematics of these excitation energies is also contained in the recent review by Vandenbosch (1973b).

Most of the experimental evidence in support of the double-humped barrier has only been indirect—in the sense of being sensitive to the *energies* of the stationary points of the potential energy surface, but not at all to their *deformation*. Information about the size of the quadrupole deformation associated with the second minimum can in principle be obtained either by determining the intrinsic quadrupole moment, or—not quite as directly—by identifying the lowest rotational band built on the isomeric ground state. Whereas no successful attempts of the former have been reported yet, our group in Munich (Specht *et al.*, 1972; Heunemann, 1972) has recently succeeded in the latter, with two further investigations being pursued in Seattle (Heffner *et al.*, 1973) and in Copenhagen (Christensen, 1973).

The principle of the experiment is briefly reviewed in Fig. 8. Following a nuclear reaction, population of excited states in the second minimum will lead to electromagnetic transitions preceding isomeric fission. Specifically in an even–even nucleus, the final decay will proceed via E2 transitions within the rotational band built on the isomeric 0^+ level. Such low-energy transitions should proceed almost entirely by internal conversion with lifetimes of the order of 5–20 psec, a time which is short compared to nearly all the fission lifetimes shown in Fig. 4. The isomeric band can therefore be identified by measuring delayed coincidences between conversion electrons and fission fragments. The results for the 4 nsec isomer in ^{240}Pu obtained from the ^{238}U $(\alpha, 2n)$ ^{240}Pu reaction which has the highest isomer production cross section known are included in Fig. 8. The observed transitions and the level scheme deduced from them are shown on the left, a fit of the transition energies to the well known expansion of the rotational energies in powers of the quantity $J \cdot (J+1)$ on the right. Whereas the rotational constant $A = 3.33$ keV found for the isomer band is less than half that for the ground-state band 7.16 keV, the "nonadiabaticity" parameter $B = -0.17$ eV shows an even stronger decrease compared to the value of -3.55 eV.

The unusually low value of the rotational constant $A = \hbar^2/2\Theta$ corresponds to the largest moment of inertia Θ ever found in nuclei and presents the only direct evidence obtained thus far that shape isomers are, in fact, connected with a nuclear deformation larger than the equilibrium ground-state deformation. In Fig. 9, the experimental moments of inertia are compared to those calculated (as a function of deformation) by Sobiczewski *et al.* (1973) on the basis of the cranking model, including the limits of the rigid rotor and the irrotational fluid. Taking a quadrupole deformation of $\epsilon_2 = 0.6$ for the second minimum the agreement with the values from the cranking model is excellent. A similar agreement is found with the results calculated by Pauli and Ledergerber, (1973). Further independent information about the size of the quadrupole deformation would, however, be needed to decide whether a pairing strength proportional to the nuclear surface area, $G \sim S$, should be preferred over a constant pairing strength, $G = $ const. In any case, the conclusion of a change in deformation appears to be rather model-independent, since the large experimental

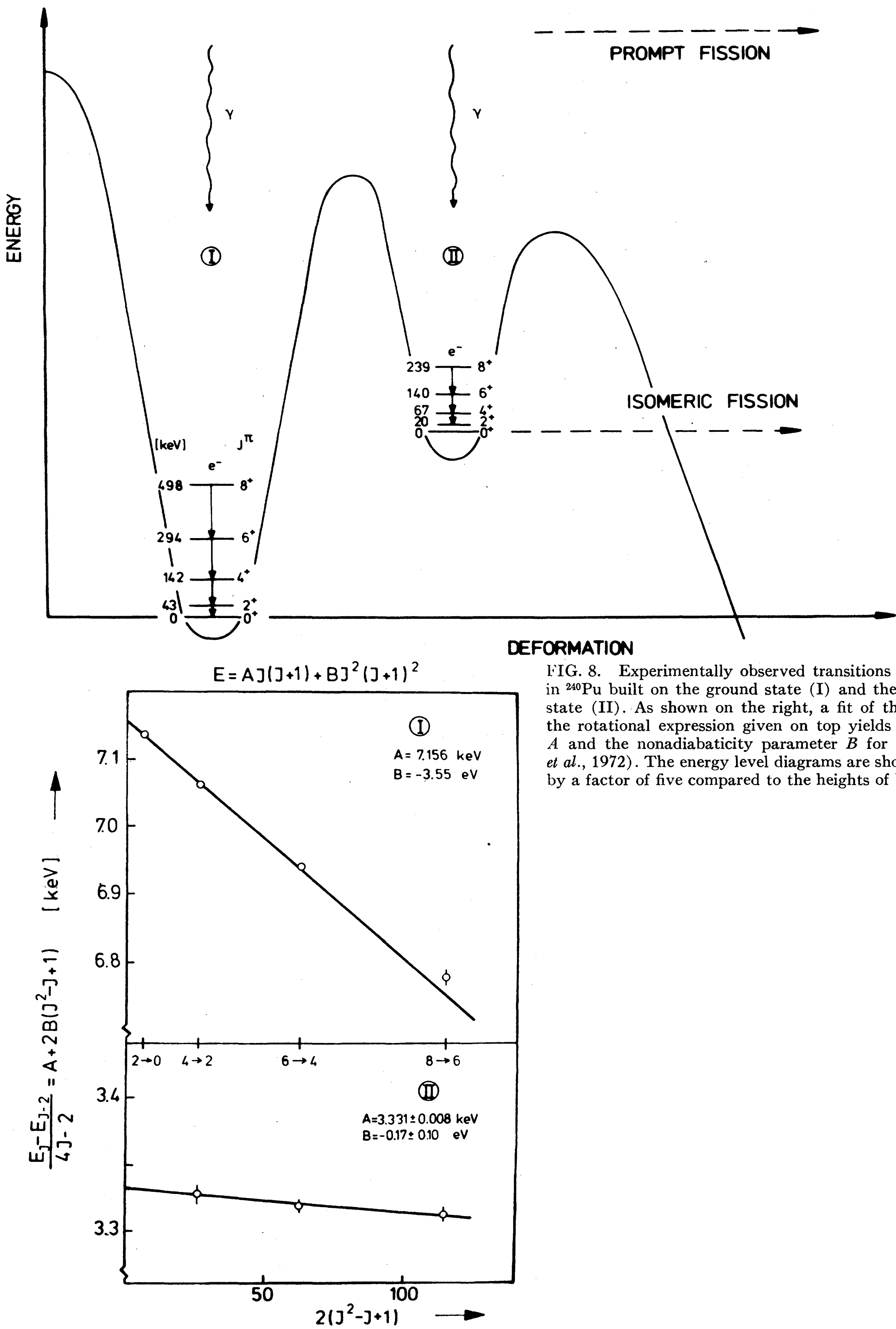

FIG. 8. Experimentally observed transitions within rotational bands in ^{240}Pu built on the ground state (I) and the 4 nsec fission-isomeric state (II). As shown on the right, a fit of the transition energies to the rotational expression given on top yields the rotational constant A and the nonadiabaticity parameter B for the two bands (Specht *et al.*, 1972). The energy level diagrams are shown on a scale expanded by a factor of five compared to the heights of barriers.

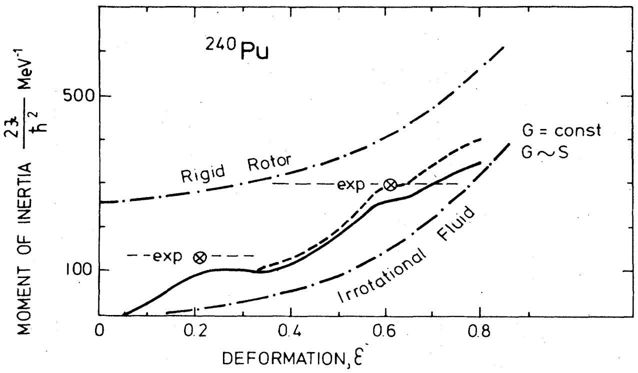

FIG. 9. Measured moments of inertia associated with rotational bands in ^{240}Pu and the calculated dependence on deformation according to the cranking model (central lines), the rigid rotor and the irrotational fluid (Sobiczewski *et al.*, 1973; Bjørnholm, 1972). The significance of G is explained in the text.

value for the moment of inertia associated with the fission isomer (horizontal line) even exceeds the rigid body limit at the ground-state deformation.

The interpretation of the strong decrease in the rotational term B, showing the shape isomer to be a "better" rotator than the ground state, presents an interesting problem in itself. It can be understood qualitatively by a decrease in the rotation–vibration or rotation–particle interaction, due to the smaller rotational energies. Alternatively, however, the observed transition energies may also be fitted to an expansion of the rotational energies in powers of the rotational frequency ω rather than angular momentum (Harris, 1965; Johnson and Szymanski, 1973), i.e., to $E = \alpha\omega^2 + \beta\omega^4$ [or, equivalently, to the two-parameter VMI model (Mariscotti *et al*, 1969)]. Interestingly, enough, the value β [or C (Mariscotti *et al.*, 1969)] is then found to be the same for the two bands, within the statistical accuracy given.

The identification of further low-lying excitations by similar techniques, measuring γ rays preceding isomeric fission, could provide information about other collective degrees of freedom in the region of the second minimum, for example about octupole or γ vibrations. Unfortunately, such measurements are even more difficult than those just described; several (unsuccessful) attempts in this direction have been reviewed elsewhere (Specht, 1973).

Could one somehow determine the quantum numbers of the isomeric ground state or low-lying excited states in odd A nuclei and thereby identify specific Nilson single-particle states in the region of the second minimum? Clearly, such information would provide a very crucial test of the parameters underlying the potential energy calculations. We have recently (Specht *et al.*, 1973) investigated projectile-fragment angular correlations in fission from isomeric states aligned by a preceding $(\alpha,2n)$ reaction. Such fragment angular distributions are uniquely determined by the spin I of the fissioning state and the quantum number K of the relevant band at the second barrier associated with the decay (Fraser and Milton, 1966). However, a reliable extraction of these quantitites from the measured data is complicated because of the degradation of the initial alignment by neutron and gamma emission prior to fission, and especially because of the possible perturbation of the correlation due to extranuclear fields (which, if turned around, might in the future yield some information about the moments of shape isomeric states).

In an attempt to circumvent this latter difficulty, we have used an implantation technique, allowing the compound nuclei to recoil into metallic Pb and identifying delayed fragments by coincidences with a pulsed beam. A parallel study with the recoiling nuclei decaying in vacuum has been performed in Dubna/Bucharest (Gangrsky *et al.*, 1972; Galeriu *et al.*, 1973). Our present angular correlation results for isomeric states in ^{237}Pu, ^{238}Pu, and ^{241}Cm are briefly reviewed in Fig. 10. In the interesting case of ^{237}Pu, two isomeric states are known to exist (Russo *et al.*, 1971), with the long-lived one (a K isomer) observed from excitation function measurements to be 0.3 MeV above the shorter-lived one (Vandenbosch *et al.*, 1973). Our preliminary and very speculative conclusions (Specht *et al.*, 1973) based on the size and the opposite sign of the anisotropies for the two states point to predominantly direct fission of the upper state. This agrees with the suggestions made earlier by Vandenbosch *et al.* (1973), on the basis of yield measurements of the two isomers as a function of angular momentum deposition in the compound nucleus (Russo *et al.*, 1971). Their tentative decay scheme (Vandenbosch, 1973b) is shown in Fig. 11; the most likely Nilsson orbitals are [615] $11/2^+$ and [862] $5/2^+$ which lie close to the Fermi surface in a number of recent calculations (Möller and Nix, 1973; Pauli, 1973; Mosel and Schmitt, 1971).

As mentioned above (Fig. 4), several even Pu isotopes also exhibit second longer-lived isomeric states above the shape isomeric ground state (Limkilde and Sletten, 1973; Metag *et al.*, 1973). They are interpreted as two-quasiparticle (neutron) excitations just above the pairing gap (Sobiczewski *et al.*, 1973; Bjørnholm, 1972; Limkilde and Sletten, 1973) with a spin $I = K$ again sufficiently high to hinder the γ decay down to the ground level via the K-selection rule. The bare existence of an anisotropy in the case of ^{238}Pu (Fig. 10) indeed supports the assumption $I = K \neq 0$ (probably ≥ 3). A comparison (Limkilde and Sletten, 1973) of the measured energy difference (1.3 ± 0.3 MeV) between the two isomeric states in this nucleus and that in similar cases in the first well shows the pairing gap at the two deformations to be approximately equal, although again no conclusion regarding the surface dependence of the pairing strength can be drawn yet (Sobiczewski *et al.*, 1973). The general retardation in the decay rates of the higher-lying states (also in ^{237}Pu) might correspond to the odd–even effect discussed above (Fig. 5), assuming conservation of the K quantum number.

Moving next to the much higher excitation energies in the vicinity of the two barrier tops, we should first discuss the status of intermediate structure in subthreshold neutron fission cross sections. The appearance of such structure, most convincingly demonstrated in the classical cases of ^{240}Pu (n,f) (Migneco and Theobald, 1968) and ^{237}Np (n,f) (Paya *et al.*, 1967, 1968), is ascribed to the coupling between the compound states of normal density in the first well to the much less dense states in the second. This picture requires resonances of only one spin to appear within each intermediate-structure group. In a very elaborate experiment using polarized neutrons on a polarized ^{237}Np target,

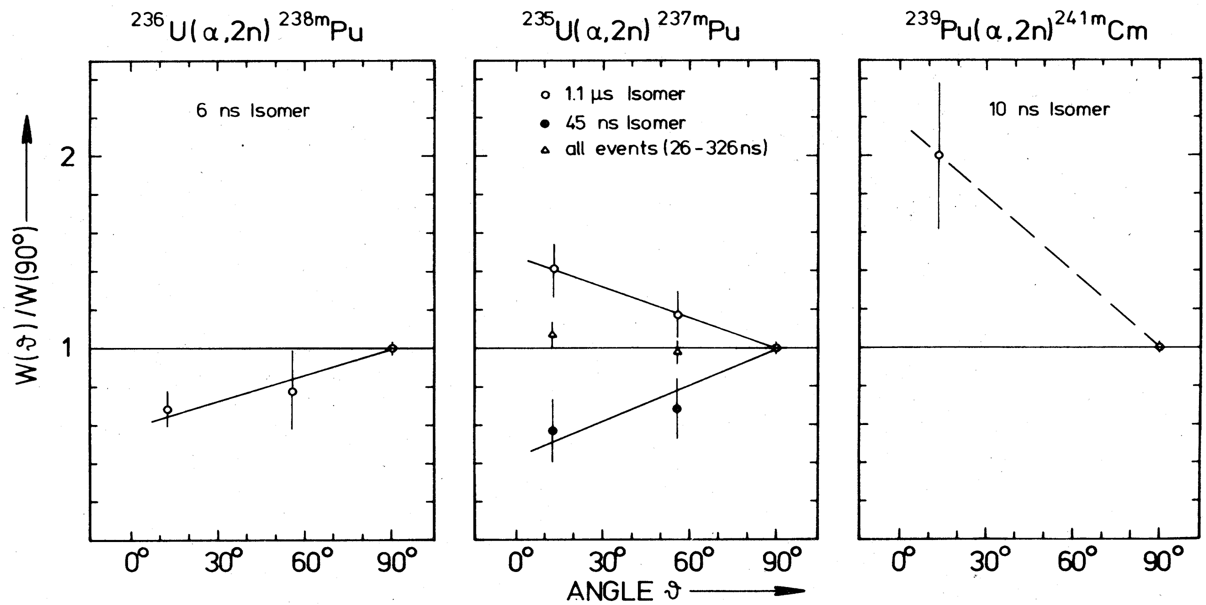

FIG. 10. Time-integral fragment angular anisotropies (relative to 90°) for isomeric states in ^{237}Pu, ^{238}Pu, and ^{241}Cm populated by the (α, $2n$) reaction (Specht *et al.*, 1973). The recoil nuclei are stopped in Pb.

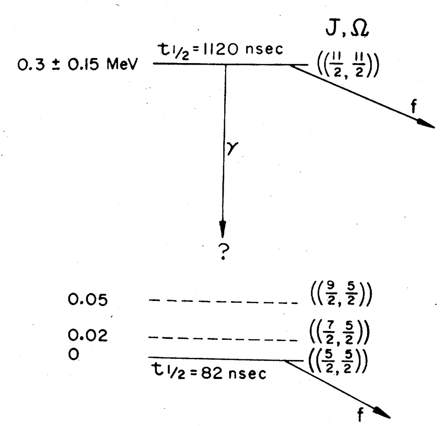

FIG. 11. Tentative decay scheme for the shape isomeric states in ^{237}Pu (Vandenbosch, 1973b).

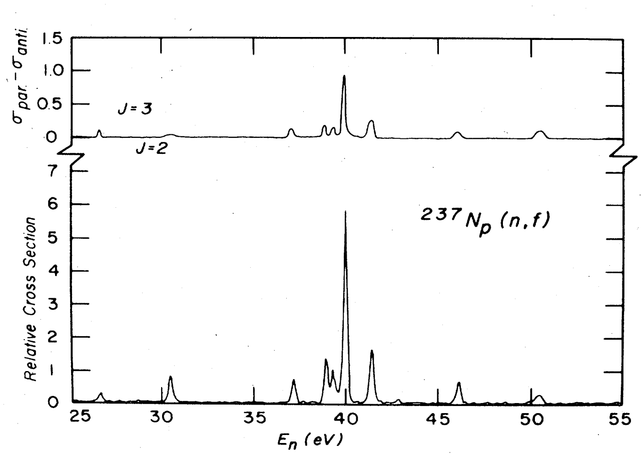

FIG. 12. Intermediate structure in the subthreshold neutron fission cross section of ^{237}Np (lower part), and differences in cross section for beam and target polarization parallel and antiparallel (upper part), indicating $I = 3$ in each case (Keyworth *et al.*, 1973).

Keyworth *et al.* at Los Alamos/Oak Ridge (1973) have indeed found all nine fine-structure resonances of the 40 eV group shown in Fig. 12 to have the same spin $I = 3^+$; in the comparison between parallel and antiparallel polarization of target and neutron spin (Fig. 12, upper part), the alternative capture spin 2^+ would fall below zero. Thus, a further beautiful piece of evidence in favor of the double-humped barrier picture has been obtained.

The heights of the two barriers themselves are most reliably determined by investigating the probability of induced fission over a range of several MeV in the threshold region. Direct reactions are the best tool for such studies: all excitation energies are obtained simultaneously in the same experiment from the kinetic energy of the outgoing particle, and the fission probability is measured directly as the ratio between the coincident fission–outgoing particle cross section and the corresponding singles cross section. Due to a long term systematic study by the Los Alamos group (Back *et al.*, 1973a and b) using (p, $p'f$), (d, pf), (t, pf), (t, αf), (^3He, df) and (^3He, αf) reactions, such probability distributions are now available for 43 isotopes from

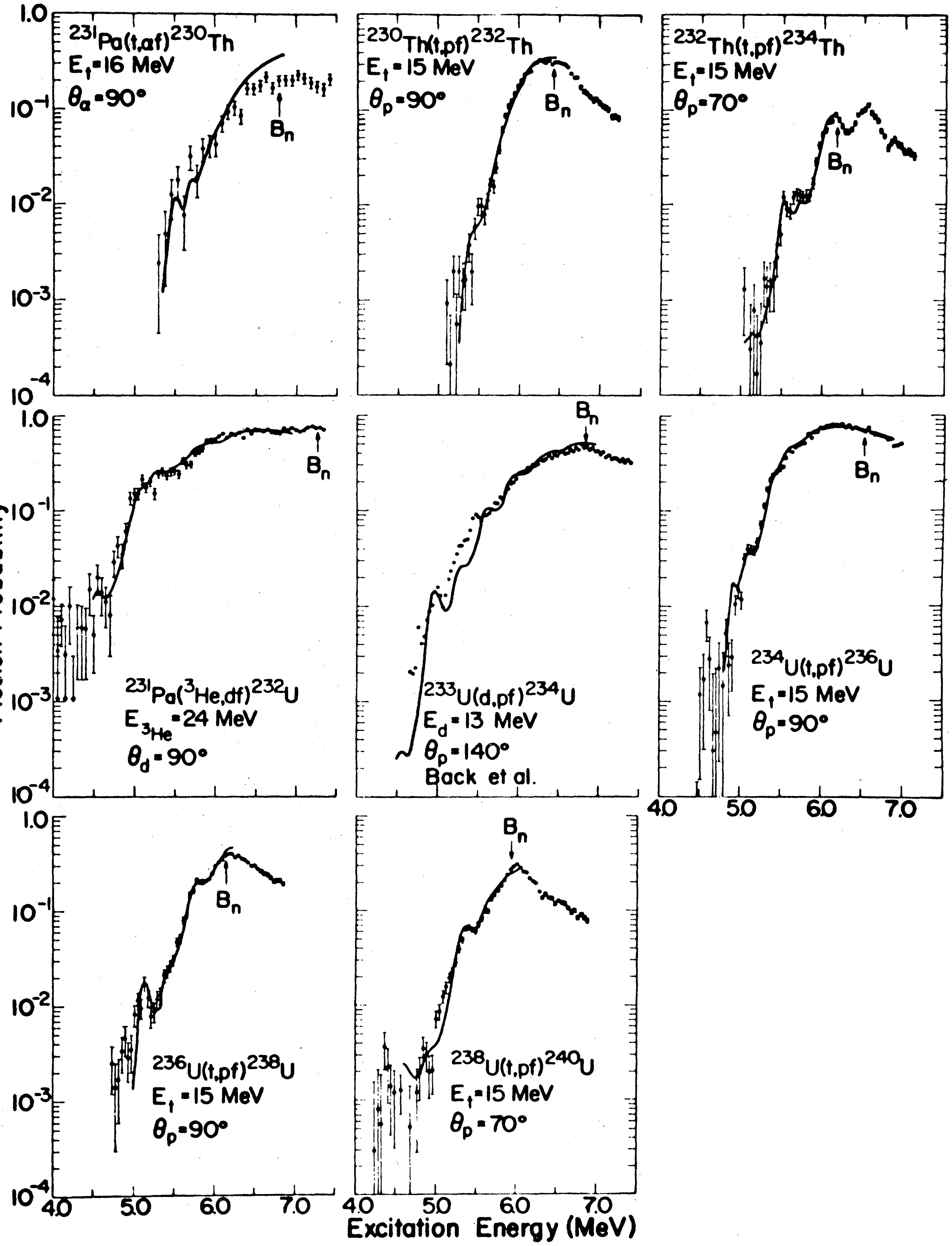

FIG. 13. Measured fission probabilities vs. excitation energy for even Th and U isotopes (data points) and statistical model fits on the basis o a one-dimensional double barrier (full lines); B_n indicates the neutron binding energy (Back *et al.*, 1973b).

Th to Bk; below this region, 11 further isotopes including Ra and Ac have been investigated in Munich (Konecny *et al.*, 1973 and unpublished data). An example for even Th and U isotopes (Back *et al.*, 1973b) is shown in Fig. 13, demonstrating the rapid rise over several orders of magnitude in the threshold region. The structure visible in most of the data is caused by transmission resonances ((Bjørnholm and Strutinsky, 1969) at the position of β-vibrational states in the second will, where the double-humped barrier acts like a classical double-layer monochromator. Approximating the barrier shape by two one-dimensional inverted parabolas, the heights and curvatures are extracted from a

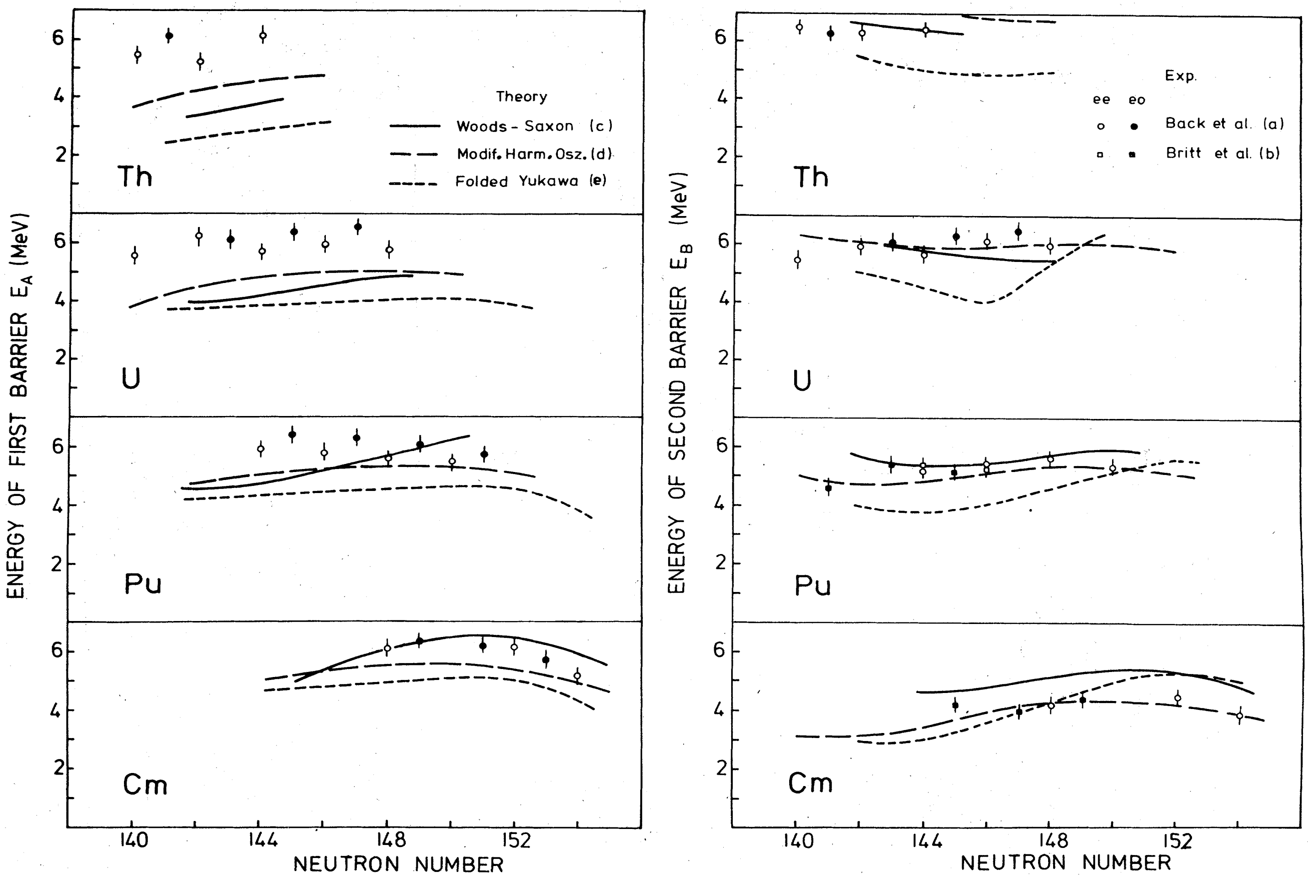

FIG. 14. Measured heights of the first and second barrier [(a) (Back *et al.*, 1973 a and b), (b) (Britt *et al.*, 1973)] as a function of neutron number and theoretical predictions from shell correction calculations based on different single particle potentials [(c) (Pauli, 1973), (d) (Möller and Nix, private communication, 1973) for E_A, (Möller and Nix, 1973; private communication, 1973) for E_B, (e) (Möller and Nix, 1973)]. Further differences are described in the text.

statistical model fit to the data, which includes competition between fission, neutron, and gamma emission in the decay of the compound nucleus and also allows for damping (Bondorf, 1970; Back *et al.*, 1971) of the resonances. The fits are shown as full lines in Fig. 13; each of the bumps corresponds to a transmission resonance with specific quantum numbers.

The heights of the first (E_A) and second (E_B) barrier deduced from this analysis (Back *et al.*, 1973a and b) and independently from fission isomer data (Britt *et al.*, 1973) are shown in Fig. 14 for even and odd isotopes of Th, U, Pu, and Cm as a function of neutron number. We have also included the latest results from three potential energy calculations, which differ mainly in the single-particle potentials employed—the Woods–Saxon ((Pauli, 1973) only the usual static barriers), the modified harmonic oscillator (Nilsson, Möller, Larsson *et al.* results for E_A from Möller and Nix, private communication, 1973; results for E_B from Möller and Nix, 1973 and Möller and Nix, private communication, 1973) and the folded Yukawa (Möller and Nix, 1973). Other differences are due to the replacement of the liquid drop by the droplet model in the latter two calculations (Möller and Nix, 1973; private communication, 1973), for which we have also included the lowering of the first barrier E_A by axially asymmetric deformations as obtained by Larsson and Leander (1973) (only approximately included for Cm in Pauli, 1973). The quite significant lowering of the second barrier E_B by mass-asymmetric deformations (see Sec. III) as well as a constant ground-state zero-point energy of 0.5 MeV were taken into account in all three calculations.

Comparing now these predictions with each other and with experiment, the over-all bandwidth of agreement appears to be of the order of 1–2 MeV. The observed systematic decrease of the second barrier with increasing Z (responsible for the disappearance of fission isomers, Fig. 4) is reproduced—perhaps not too surprisingly, since it is basically caused by the behavior of the liquid drop barrier. Definite difficulties remain at the first barrier E_A for U and especially Th, where the theoretical predictions tend to lie low and also decrease too rapidly with decreasing Z. Several suggestions have been made (Möller and Nix, 1973; Pauli and Ledergerber, 1973) to solve this much cited "Th-anomaly"; it is an open problem. The discrepancy seems to be not quite so severe for Nilsson's modified harmonic oscillator calculations—which, in fact, show the best over-all agreement with experiment also with regard to the finer details of the neutron number dependences. A more exten-

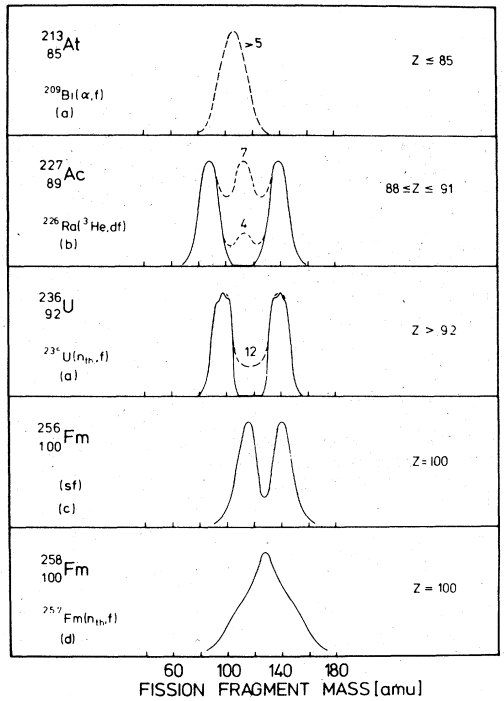

FIG. 15. Representative fragment mass distributions in low-energy fission (full lines) and their dependence on excitation energy above the barrier (in MeV, dashed lines) and atomic number for first chance fission [(from (a) (Hyde, 1964), (b) (Konecny *et al.*, 1973), (c) (Unik *et al.*, 1973), and (d) (John *et al.*, 1973; Ragaini *et al.*, 1973)].

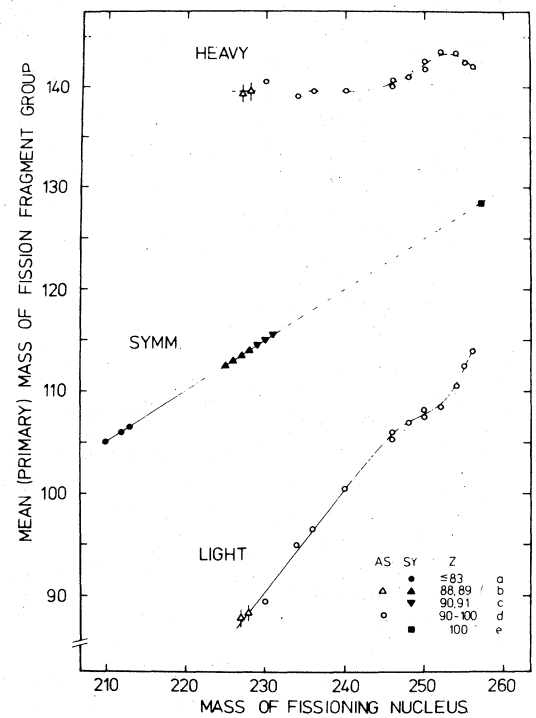

FIG. 16. Mean primary masses of the light and heavy fragment group in asymmetric fission as a function of fissioning mass at low excitation energies ($\leq$ 1 MeV above the barrier). Points on the straight line for symmetric fission correspond to observed central maxima at larger excitation energies [data from (a) (Hyde, 1964), (b) (Konecny *et al.*, 1973), (c) (Britt *et al.*, 1963), (d) (Unik *et al.*, 1973), and (e) (John *et al.*, 1971; Ragaini *et al.*, 1973)].

sive comparison of all these results (including the height of the second minimum) can be found in a review by Nix (Möller and Nix, 1973).

III. THE MASS-ASYMMETRY OF THE BARRIER

Our next major topic is a discussion of the long-standing puzzle of fragment mass distribution in nuclear fission and the present status of their understanding. Fig. 15 reviews the appearance of these distributions as a function of atomic number and excitation energy; the representative nuclei are listed on the left, the regions of occurrence on the right. The full lines correspond to low-energy fission, i.e., either spontaneous or induced fission with excitation energies <1 MeV above the barrier, the dashed lines signify the change in the distributions at larger excitation energies. As has been known for many years (Hyde, 1964), nuclei with $Z \leq 83$ fission symmetrically (reasonably well described by the liquid drop model, Nix and Swiatecki, 1965), the heavier actinides asymmetrically. The example of ^{227}Ac (Konecny *et al.*, 1973) illustrates the transition between these two extremes. Measurements of such triple-humped mass distributions in the region from $Z = 88$ to at least 91 (Jensen and Fairhall, 1958, 1960; Britt *et al.*, 1963; Konecny and Schmitt, 1968; Perry and Fairhill, 1971; Konecny *et al.*, 1973), systematic differences in fragment total kinetic energies and their variances (Britt *et al.*, 1963; Konecny and Schmitt, 1968; Perry and Fairhall, 1971; Konecny *et al.*, 1973), also found for $Z > 91$ (Hyde, 1964; Britt and Whetstone, 1964; Ferguson *et al.*, 1973), and finally prompt neutron emission (Konecny and Schmitt, 1968), appear to indicate that the "two fission modes" (Niday, 1961) coexist in the same nucleus. The relative probability of the symmetrical component seems to decrease only gradually with increasing mass number, but always increases exponentially with excitation energy with a slope nearly independent of Z. We shall return to this interesting competition later. For very heavy nuclei, the smoothly decreasing mass asymmetry finally causes the symmetrical valley to fill in again even at low excitation energies, i.e., for the lighter Fm isotopes (Balagna *et al.*, 1971; John *et al.*, 1971; Ragaini *et al.*, 1973; Unik *et al.*, 1973), until at ^{258}Fm (John *et al.*, 1971; Ragaini *et al.*, 1973) a new and different type of symmetric fission occurs, characterized by a maximum in the total fragment kinetic energy rather than a minimum as before.

The well known (Hyde, 1964) constancy of the heavy mass group and the very smooth shift of the light one with increasing mass of the fissioning nucleus is shown more quantitatively in Fig. 16. With the exception of the low-energy points for Ac isotopes (Konecny *et al.*, 1973), only new data from Unik *et al.* (1973) with a very high relative precision ($\pm$0.2 amu) have been plotted. Points on the straight line for symmetric fission correspond to those cases, where a central maximum in the mass distribution at larger excitation energies (except for ^{258}Fm) has clearly been identified. The exact boundaries of the overlap region of the two "modes" are not known yet, the lower limit at present is ^{225}Ra (Konecny *et al.*, 1973), but it appears that asymmetric fission sets in suddenly with a maximum degree of asymmetry.

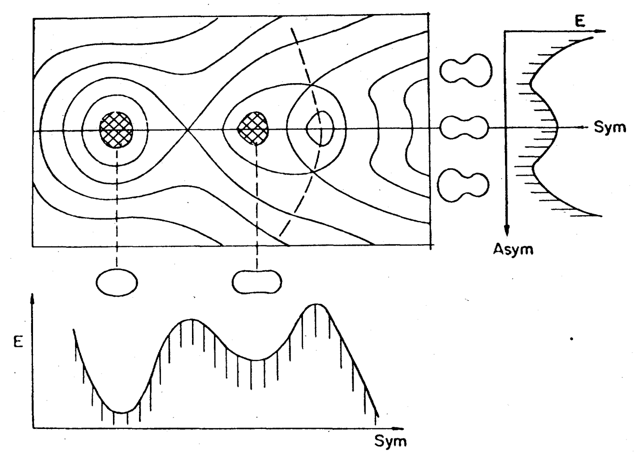

FIG. 17. Schematic illustration of the nuclear potential energy surface as a function of symmetric (ϵ_2) and asymmetric (ϵ_3) deformations (Tsang and Wilhelmy, 1972).

What then is the interpretation of this asymmetry? It is now understood as a preference of actinide nuclei to move in regions of mass-asymmetric shell valleys, starting already at the second barrier. Following old suggestions by Inglis (1958) and Johansson (1961), the lowering of the second barrier by such octupole (pearshape-like) distortions was first demonstrated on the basis of Strutinski-type calculations by Möller and Nilsson (1970; Möller, 1972), and later confirmed by several other groups (Pashkevich, 1971; Pauli *et al.*, 1971; Bolsterli *et al.*, 1972; Mustafa *et al.*, 1973; Pauli and Ledergerber, 1973). As illustrated by the schematic ϵ_2/ϵ_3 potential energy surface in Fig. 17 (Tsang and Wilhelmy, 1972), this instability occurs only at the outer saddle, not at the inner one or the two minima. The dependence of the energy on the octupole deformation ϵ_3 (cut "Asym" along the dotted line) resembles that of the familiar NH_3 molecule. The calculated energy gain is of the order of 0–3 MeV. It originates from only a few strongly interacting Nilsson orbitals of opposite parity in the vicinity of the Fermi surface which move down in energy with increasing asymmetric deformation, thus reducing the large level density and with it the large positive shell correction energy associated with the second barrier (Gustafson *et al.*, 1971; Möller, 1972); the symmetry-favoring liquid drop energy increases sufficiently slowly not to destroy the effect. As an example, Fig. 18 shows the potential energy surface for ^{238}U, calculated by Mosel *et al.* (Mustafa, Mosel, and Schmitt, 1973) with the two-center harmonic oscillator potential. Contours of constant energy (in MeV) are plotted as a function of the mass asymmetry and the neck radius of the fissioning system. The asymmetrically deformed outer barrier (at $D = 5$ fm) is similar to what is obtained by all the other calculations. The attractive result, however, of an apparent shell valley extending from the saddle all the way down to scission (at $D = 0$) with a nearly constant mass asymmetry (see also Pauli, 1973; Pauli and Ledergerber, 1973) is a matter of some controversy. Other investigations (Möller and Nix, 1973) not minimizing the energy with respect to elongation (as in Mustafa *et al.*, 1973) have shown fluctuations between different valleys in the saddle to scission stage.

Direct experimental evidence supporting the asymmetric shape of the second barrier is virtually nonexistent. The

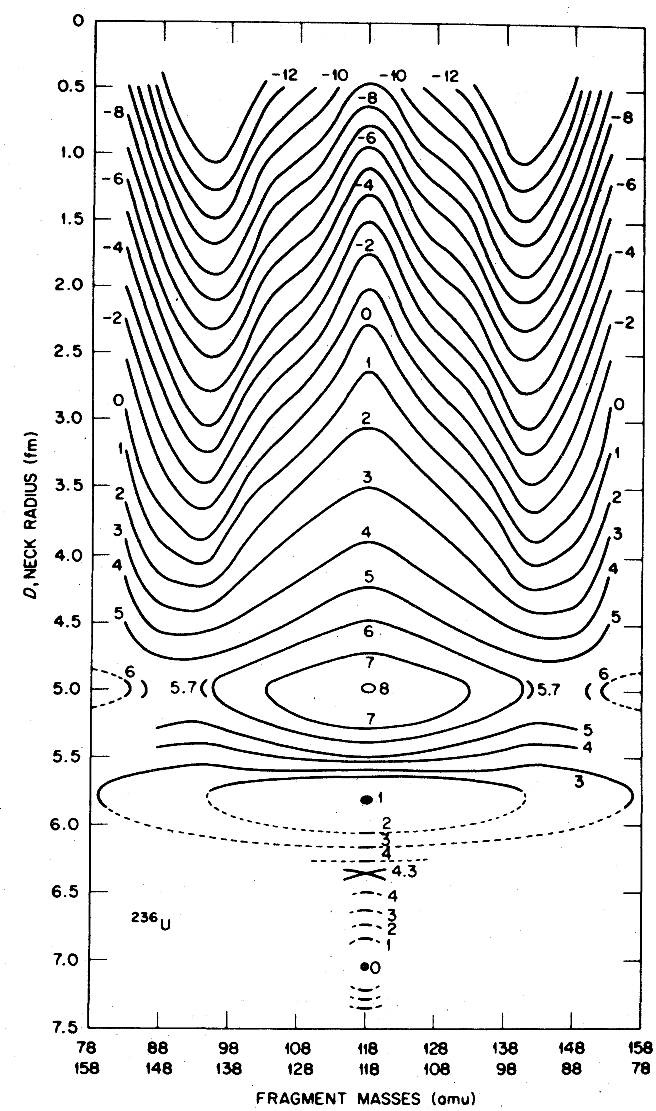

FIG. 18. Potential energy surface of ^{236}U, calculated by Mustafa, Mosel, and Schmitt (1973). Contours of constant energy (in MeV) are shown as a function of the mass asymmetry and the neck radius of the fissioning system.

agreement between the measured and predicted barrier heights E_B (Fig. 14) is comfortable, but certainly no proof in view of the difficulties at the inner saddle. Better evidence stems from near-threshold photofission results, where the ratio of the quadrupole to the dipole component increases very rapidly from Th to Pu (see Vandenbosch, 1973a for details).

If one accepts the point of view that the gross character of the fragment mass split is already predetermined at the outer barrier (Johansson, 1961; Möller and Nilsson, 1970; Pashkevich, 1971; Pauli *et al.*, 1971; Bolsterli *et al.*, 1972; Möller and Nix, 1973; Pauli, 1973; Möller, 1972; Pauli and Ledergerber, 1973), essentially unchanged by either a change in the static surface or by dynamics (Pauli and Ledergerber, 1973; Maruhn *et al.*, 1973), then there should again be observable consequences. We will discuss two of them—the correlation between the experimentally observed fragment mass ratio and the calculated size of the octupole

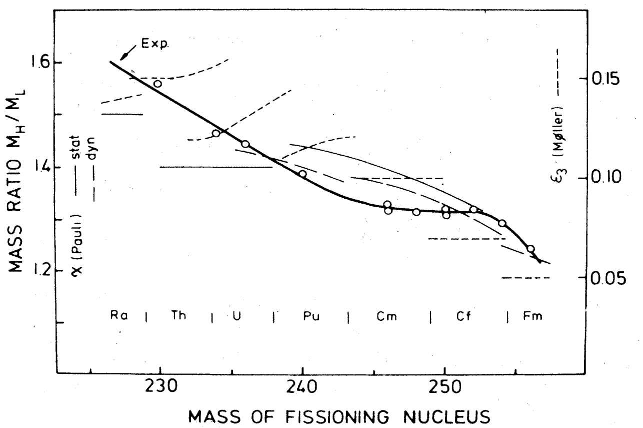

FIG. 19. The ratio of the measured mean primary masses in the two fragment groups as a function of the fissioning mass (data from Fig. 16) compared to theoretical predictions of the closely related quantity χ [at static (Pauli *et al.*, 1971; Pauli, 1973) and dynamic barrier (Pauli and Ledergerber, 1973)], and the octupole deformation ϵ_3 (Möller, 1972), respectively.

distortion at the second barrier,—and the possible existence of different barriers for symmetric and asymmetric fission.

In a way slightly different from previous correlation diagrams (Möller and Nix, 1973; Möller, 1972; Pauli and Ledergerber, 1973), we have plotted in Fig. 19 the experimentally observed ratio of the mean primary masses in the two fragment groups versus mass of the fissioning nucleus, taken from the data of Fig. 16 (data points shown only for doubly even nuclei). We have included the theoretical predictions for the closely related quantity χ by Pauli *et al.* at the static (1971; Pauli, 1973) and the dynamic (Pauli and Ledergerber, 1973) outer barrier, and those for the octupole deformation ϵ_3 given by Möller (1972); the scale factor for the latter was arbitrarily chosen such as to resemble the mass ratio on the average. The over-all trend of this ratio decreasing rapidly from Th to Fm is definitely reproduced by all the calculations, including the final transition to symmetry for very heavy elements (see also Möller and Nix, 1973; Mustafa *et al.*, 1973). However, there is no detailed agreement and one is probably not to be expected from such a simple static picture. Neither the exact location of this transition, nor the rather constant ratio in the Cm/Cf region, nor the extremely smooth experimental trend is found. The neutron number dependence for the lighter actinides obtained from the modified harmonic oscillator calculations (Möller, 1972) is, in fact, opposite to observation (slightly improved in the newest version) (Möller and Nix, private communication, 1973). Such difficulties for the lighter actinides also appear to exist in the folded Yukawa calculations (Möller and Nix, 1973). In the region of symmetrical fission for $Z < 83$ (Fig. 15), indeed a symmetrical saddle (or at least an extremely flat potential energy surface) is found in most of the calculations, the liquid drop behavior overriding the shell effects. A specific problem, however, arises in the whole region of coexistence of the two modes—there are at most slight hints (Pauli, 1973; Möller, 1972) for the possible existence of two different saddles, i.e., an asymmetrical potential energy curve (Fig. 17) with an additional central minimum.

In order to study this unsettled question of different barriers for symmetric and asymmetric fission as well as the detailed competition between the two modes, we have recently measured in Munich, separately for the two mass components, fission probability distributions and fragment anisotropies, presumed to be determined at the barrier, for a whole series of nuclei in this critical triple-humped region (Konecny *et al.*, 1973). A decision about different saddles is hardly feasible in higher Z actinide nuclei because of the inner barrier being the higher one (Fig. 14). Using again direct reactions as described in connection with Fig. 13, the energies of the outgoing light particles, identified by an $\Delta E - E$ telescope, were recorded in coincidence with the energies of both fragments, measured in two pairs of detectors at 0° and 90° relative to the recoil axis; from the energies, fragment masses are obtained in the usual way via mass and momentum conservation. As an example from this work Fig. 20 shows, for both modes, fission probabilities and fragment anisotropies versus excitation energy in the final nuclei ^{226}Ac, ^{227}Ac, and ^{228}Ac, respectively. In the following we will briefly discuss two interesting features directly visible in this plot.

First and most important, symmetric and asymmetric fission appear, in fact, to be associated with different fission barriers, at least for these odd nuclei. In the cases of ^{227}Ac and ^{228}Ac, the symmetric barrier is higher than the asymmetric one by 1.2 and 2.0 MeV, respectively; the upper limit for a possible symmetric yield averaged over the region between the two thresholds relative to the symmetric yield just above the symmetric threshold is 3%, with a 95% confidence limit. The structure seen in the asymmetric component of ^{227}Ac in this region is possibly caused by the competing neutron channel. The fragment angular anisotropies also seem to be different for the two modes, further supporting the interpretation of the different threshold behavior as really being due to separate barriers.

Second the fission probability for the asymmetric component, although very small compared to the distributions in Fig. 13, increases—beyond the usual rapid rise at the threshold—much more slowly with increasing excitation energy than expected on the basis of simple statistical model considerations (Huizenga and Vandenbosch, 1962) for the competition of fission and neutron emission; the increase above the dotted line for ^{228}Ac is caused by the onset of second chance fission, i.e., fission following evaporation of a neutron from the compound nucleus. The competition between the two modes, on the other hand, is governed by a steep exponential rise of the symmetric component with a relative slope nearly identical to that found in higher Z actinide nuclei [$\sim$0.5 MeV^{-1} for $\ln(\Gamma_{f\ \mathrm{sym}}/\Gamma_{f\ \mathrm{asym}})$]; it becomes smaller only for the very neutron-poor isotopes investigated (^{226}Ac, ^{225}Ra), where the fraction of symmetry is highest. In the case of ^{228}Ac [also for ^{225,227}Ra (Konecny *et al.*, 1973)], the symmetrical yield even exceeds the asymmetric one at excitation energies only a few MeV above the barrier. This remarkable result as well as the general rapid rise of symmetry close to threshold can apparently not be explained by a "washing-out" of shell effects with increasing excitation energy, which according to several recent calculations of this temperature dependence (Moretto, 1972; Jensen and Damgaard, 1973; Jensen and Dössing, 1973; Schmitt and Mustafa, 1973; Maruhn *et al.*, 1973) should only become operative at much higher energies; in

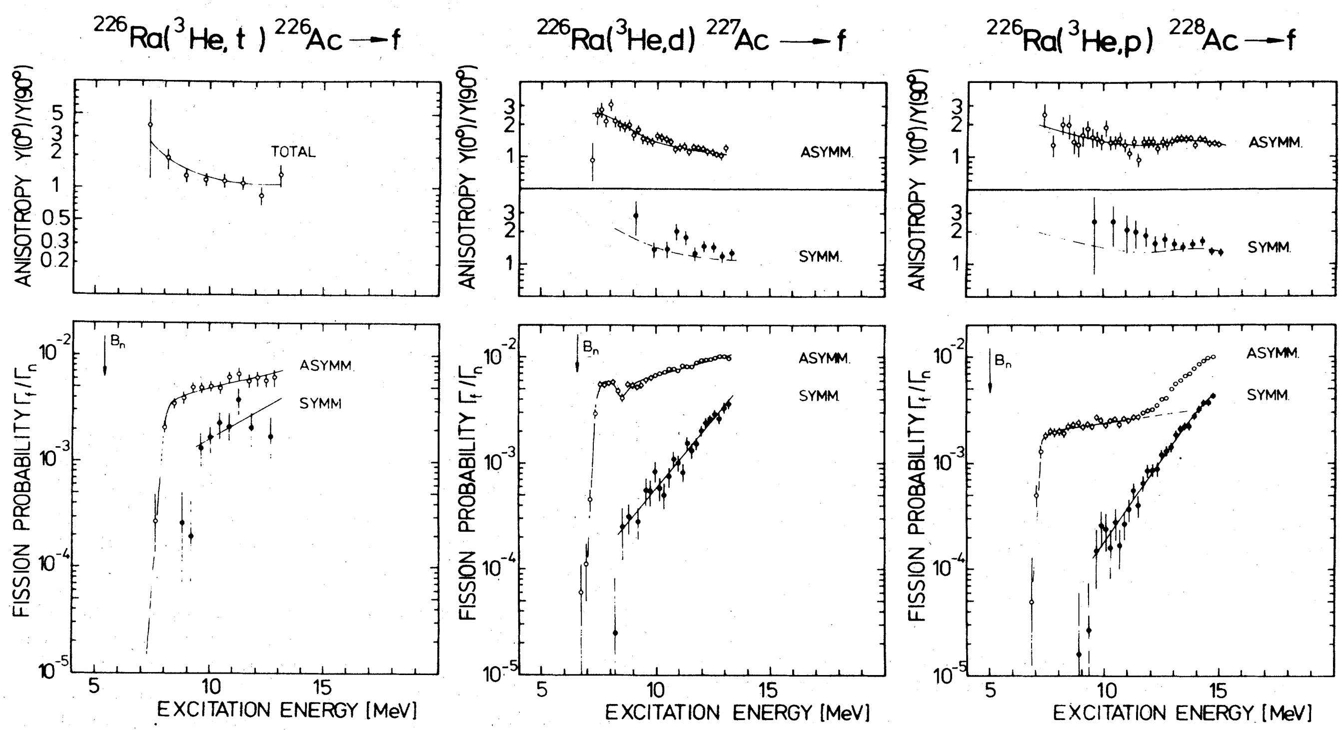

FIG. 20. Fission probabilities and fragment anisotropies versus excitation energy in the fissioning nuclei ^{226,227,228}Ac, for the symmetric and the asymmetric mass component separately. The neutron binding energy B_n is marked by an arrow. The solid lines drawn through the asymmetric anisotropy data are shown as dashed lines in the data fields for symmetry.

that region, the experimental findings including the observed decrease in the size of the asymmetry (Jensen and Damgaard, 1973; Jensen and Dössing, 1973; Ferguson *et al.*, 1973) are reproduced. The somewhat equivalent consideration of level densities at the two different outer saddles controlling the competition would require differences in the level density parameter between 20% and 40% (depending on the nucleus).

Thus, there are difficulties. Although the existence of different barriers for the two fission components is seemingly in accord with the expectations from shell model calculations, it is not at all clear at the moment, how the sole occurrence of triple-humped mass distributions and the detailed competition between the two modes including the "cross-over" observed should be understood on the basis of the barrier shapes calculated so far.

IV. CONCLUSION

We will summarize our findings quite briefly. Experimental evidence supporting the double-humped barrier picture has been accumulating rapidly in the last few years, and in several respects nearly quantitative agreement is found with theoretical predictions, although some difficulties remain. As far as the understanding of fragment mass distributions is concerned, however, there are still major open problems.

ACKNOWLEDGMENTS

It is a pleasure to acknowledge useful discussions with Dr. S. Bjørnholm, Dr. K. Dietrich, Dr. W. Greiner, Dr. P. Kienle, Dr. E. Konecny, Dr. S. G. Nilsson, Dr. J. R. Nix, Dr. W. Nörenberg, Dr. H. C. Pauli, and Dr. R. Vandenbosch. I also would like to thank Dr. P. Möller and Dr. J. R. Nix for sending their latest results prior to publication.

REFERENCES

Back, B. B., J. P. Bondorf, G. A. Ostroschenko, J. Pedersen, and B. Rasmussen, 1971, Nucl. Phys. A **165**, 449.

Back, B. B., H. C. Britt, J. D. Garrett, O. Hansen, and B. Leroux, 1973a, IAEA Third Symp. Phys. and Chem. of Fission, Rochester (Paper SM-174/201).

Back, B. B., O. Hansen, H. C. Britt, and J. D. Garrett, 1973b, IAEA Third Symp. Phys. and Chem. of Fission, Rochester (Paper SM-174/27).

Balagna, J. P., G. P. Ford, D. C. Hoffmann, and J. D. Knight, 1971, Phys. Rev. Lett. **26**, 145.

Bjørnholm, S., 1972, EPS Conf. Nucl. Phys., Aix-en-Provence [J. Phys. (Paris), Series des Colloques **33**, C5–33].

Bjørnholm, S., and V. M. Strutinski, 1969, Nucl. Phys. A **136**, 1.

Bolsterli, M., E. O. Fiset, J. R. Nix, and J. L. Norton, 1972, Phys. Rev. C **5**, 1050.

Bondorf, J. P., 1970, Phys. Lett. B **31**, 1.

Brack, M., J. Damgaard, H. C. Pauli, A. S. Jensen, V. M. Strutinski, and C. Y. Wong, 1972, Rev. Mod. Phys. **44**, 320.

Brack, M., and P. Quentin, 1973, IAEA Third Symp. Phys. and Chem. of Fission, Rochester (Paper SM-174/98).

Britt, H. C., 1973, Atomic and Nuclear Data Tables 12, 407.

Britt, H. C., M. Bolsterli, J. R. Nix, and J. L. Norton, 1973, Phys. Rev. C **7**, 801.

Britt, H. C., H. E. Wegner, and J. C. Gursky, 1963, Phys. Rev. **129**, 2239.

Britt, H. C., and S. L. Whetstone, 1964, Phys. Rev. B **133**, 603.

Christensen, J., 1973, Niels Bohr Institute, Copenhagen (private communication).

Ferguson, R. L., F. Plasil, F. Pleasonton, S. C. Burnett, and H. W. Schmitt, 1973, Phys. Rev. C **7**, 2510.

Flocard, H., P. Quentin, D. Vautherin, and A. K. Kerman, 1973, IAEA Third Symp. Phys. and Chem. of Fission, Rochester (Paper SM-174/38).
Fraser, J. S., and J. C. D. Milton, 1966, Ann. Rev. Nucl. Sci. **16**, 379 (see for a review of the underlying formalism).
Galeriu, D., *et al.*, 1973, IAEA Third Symp. Phys. and Chem. of Fission, Rochester (Paper SM-174/15).
Gangrsky, J. P., N. C. Khanh, D. D. Pulatov, and P. Z. Hien, 1972, preprint (Dubna P7-6466).
Gustafson, C., P. Möller, and S. G. Nilsson, 1971, Phys. Lett. B **34**, 349.
Harris, S. M., 1965, Phys. Rev. B **138**, 509.
Heffner, R., J. Pedersen, P. A. Russo, G. Sletten, and H. Swanson, 1973, Nucl. Phys. Lab. Ann. Rep. (University of Washington, Seattle, Washington), p. 123.
Heunemann, D., 1972, dissertation (Technische Universität München).
Huizenga, J. R., and R. Vandenbosch, 1962, in *Nuclear Reactions*, edited by P. M. Endt and P. B. Smith (North-Holland, Amsterdam, 1962), Vol. 2.
Hyde, E. K., 1964, *The Nuclear Properties of the Heavy Elements* (Prentice-Hall, New York, 1964), Vol. 3.
Inglis, D. R., 1958, Ann. Phys. **5**, 106.
Jensen, A. S., and J. Damgaard, 1973, Nucl. Phys. A **203**, 578.
Jensen, A. S., and J. Damgaard, 1973, Nucl. Phys. A **210**, 282.
Jensen, A. S., and T. Dössing, 1973, IAEA Third Symp. Phys. and Chem. of Fission, Rochester (Paper SM-174/28).
Jensen, R. C., and A. W. Fairhall, 1958, Phys. Rev. **109**, 942.
Jensen, R. C., and A. W. Fairhall, 1960, Phys. Rev. **118**, 771.
Johansson, S. A. E., 1961, Nucl. Phys. **22**, 529.
Johansson, T., S. G. Nilsson, and Z. Szymanski, 1970, Ann. Phys. (Paris) **5**, 377.
John, W., E. K. Hulet, R. W. Lougheed, and J. J. Wesolowski, 1971, Phys. Rev. Lett. **27**, 45.
Johnson, A., and Z. Szymanski, 1973, Phys. Rep. **7**, 181.
Keyworth, G. A., J. R. Lemley, C. E. Olsen, F. T. Seibel, J. W. T. Dabbs, and N. W. Hill, 1973, IAEA Third Symp. Phys. and Chem. of Fission, Rochester (Paper SM-174/65).
Konecny, E., and H. W. Schmitt, 1968, Phys. Rev. **172**, 1213; 1226.
Konecny, E., H. J. Specht, and J. Weber, 1973, IAEA Third Symp. Phys. and Chem. of Fission, Rochester (Paper SM-174/20).
Konecny, E., H. J. Specht, and J. Weber, 1973, Phys. Lett. B **45**, 329 (and unpublished data).
Larsson, S. E., and G. Leander, 1973, IAEA Third Symp. Phys. and Chem. of Fission, Rochester (Paper SM-174/6).
Limkilde, P., and G. Sletten, 1973, Nucl. Phys. A **199**, 504.
Mariscotti, M. A. I., G. Scharff-Goldhaber, and B. Buck, 1969, Phys. Rev. **178**, 1864.
Maruhn, J., W. Greiner, P. Lichtner, and D. Drechsel, 1973, IAEA Third Symp. Phys. and Chem. of Fission, Rochester (Paper SM-174/102).
Maruhn, J., W. Greiner, P. Lichtner, and D. Drechsel, 1973, Phys. Lett. B **45**, 175.
Metag, V., E. Liukkonen, O. Glomset, and A. Bergman, 1973, IAEA Third Symp. Phys. and Chem. of Fission, Rochester (Paper SM-174/26).
Migneco, E., and J. P. Theobald, 1968, Nucl. Phys. A **112**, 603.
Möller, P., 1972, Nucl. Phys. A **192**, 529.
Möller, P., and S. G. Nilsson, 1970, Phys. Lett. B **31**, 283.
Möller, P., and J. R. Nix, 1973 (private communication).
Möller, P., and J. R. Nix, 1973, IAEA Third Symp. Phys. and Chem. of Fission, Rochester (Paper SM-174/202).
Moretto, L. G., 1972, Nucl. Phys. A **180**, 337.
Moretto, L. G., 1972, Nucl. Phys. A **182**, 641.
Mosel, U., and H. W. Schmitt, 1971, Nucl. Phys. A **165**, 13.
Mustafa, M. G., U. Mosel, and H. W. Schmitt, 1973, Phys. Rev. C **7**, 1519.
Niday, J. B., 1961, Phys. Rev. **121**, 1471.
Nix, J. R., 1972, Ann. Rev. Nucl. Sci. **22**, 65.
Nix, J. R., and W. J. Swiatecki, 1965, Nucl. Phys. **71**, 1.
Nix, J. R., and G. E. Walker, 1969, Nucl. Phys. A **132**, 60.
Pashkevich, V. V., 1971, Nucl. Phys. A **169**, 275.
Pauli, H. C., 1973, Phys. Rep. **7**, 35.
Pauli, H. C., and T. Ledergerber, 1973, Nucl. Phys. A **207**, 1.
Pauli, H. C., and T. Ledergerber, 1973, IAEA Third Symp. Phys. and Chem. of Fission, Rochester (Paper SM-174/206).
Pauli, H. C., T. Ledergerber, and M. Brack, 1971, Phys. Lett. B **34**, 264.
Paya, D., H. Derrien, A. Fubini, A. Michaudon, and P. Ribon, 1967, *Nuclear Data for Reactors* (IAEA, Vienna, 1967) Vol. II, p. 128.
Paya, D., H. Derrien, A. Fubini, A. Michauden, and P. Ribon, 1968, Phys. Rev. Lett. **20**, 1373.
Perry, D. G., and A. W. Fairhall, 1971, Phys. Rev. C **7**, 977.
Polikanov, S. M., V. A. Druin, V. A. Karnaukhov, V. L. Mikheev, A. A. Pleve, N. K. Skobelev, V. G. Subbotin, G. M. Ter-Akopjan, and V. A. Fomichev, 1962, Sov. Phys.—JETP **15**, 1016.
Ragaini, R. C., E. K. Hulet, R. W. Lougheed, and J. Wild, 1973, Phys. Rev. C (to be published).
Russo, P. A., J. Pedersen, and R. Vandenbosch, 1973, IAEA Third Symp. Phys. and Chem. of Fission, Rochester (Paper SM-174/96).
Russo, P. A., R. Vandenbosch, M. Mehta, J. R. Tesmer, and K. L. Wolf, 1971, Phys. Rev. C **3**, 1595.
Schmitt, H. W., and M. G. Mustafa, 1973, IAEA Third Symp. Phys. and Chem. of Fission, Rochester (Paper SM-174/73).
Schütte, G., and L. Wilets, 1973, IAEA Third Symp. Phys. and Chem. of Fission, Rochester (Paper SM-174/210).
Sobiczewski, A., S. Bjørnholm, and K. Pomorski, 1973, Nucl. Phys. A **202**, 274.
Specht, H. J., 1973, Proc. Minerva Symp. Phys. (Rehovot). Lecture Notes in Physics, **23**, 105 (Springer, Berlin, Heidelberg, New York, 1973).
Specht, H. J., E. Konecny, J. Weber, and C. Kozhuharov, 1973, IAEA Third Symp. Phys. and Chem. of Fission, Rochester (Paper SM-174/19).
Specht, H. J., J. Weber, E. Konecny, and D. Heunemann, 1972, Phys. Lett. B **41**, 43.
Strutinski, V. M., 1966, Yad. Fiz. **3**, 614.
Strutinski, V. M., 1966, Sov. J. Nucl. Phys. **3**, 449.
Strutinski, V. M., 1967, Nucl. Phys. A **95**, 420.
Strutinski, V. M., 1968, Nucl. Phys. A **122**, 1.
Tsang, C. F., and J. B. Wilhelmy, 1972, Nucl. Phys. A **184**, 417.
Unik, J. P., J. E. Gindler, L. E. Glendenin, K. F. Flynn, A. Gorski, and R. K. Sjoblom, 1973, IAEA Third Symp. Phys. and Chem. of Fission, Rochester (Paper SM-174/209).
Vandenbosch, R., 1973a, Phys. Lett. B **45**, 207.
Vandenbosch, R., 1973b, IAEA Third Symp. Phys. and Chem. of Fission, Rochester (Paper SM-174/203).
Vandenbosch, R., P. A. Russo, G. Sletten, and M. Mehta, 1973, Phys. Rev. C **8**, 1080.
Vautherin, D., 1973, Int. Conf. Nucl. Phys. (Munich), Vol. 2.
Wieczorek, R., R. W. Hasse, and G. Süssmann, 1973, IAEA Third Symp. Phys. and Chem. of Fission, Rochester (Paper SM-174/2).
Wong, C. Y., 1970, Phys. Lett. B **32**, 668.